American Journal of Analytical Chemistry, 2025, 16(8), 174-184
https://www.scirp.org/journal/ajac
ISSN Online: 2156-8278
ISSN Print: 2156-8251

Spectral Characterization of 4-Mercaptopyridine (4-Mpy) Aggregates in Aqueous Solution

Syed K. Islam, Neema B. Rock

Department of Physical Sciences, Eastern Connecticut State University, Willimantic, USA
Email: islams@easternct.edu

How to cite this paper: Islam, S.K. and Rock, N.B. (2025) Spectral Characterization of 4-Mercaptopyridine (4-Mpy) Aggregates in Aqueous Solution. *American Journal of Analytical Chemistry*, **16**, 174-184.
https://doi.org/10.4236/ajac.2025.168011

Received: July 24, 2025
Accepted: August 12, 2025
Published: August 15, 2025

Abstract

This study investigates the spectroscopic characteristics of 4-mercaptopyridine (4-Mpy) molecular aggregates formed in aqueous solution. Due to their low solubility in water, 4-Mpy molecules undergo solution-driven aggregation, which results in a blue shift in their absorption maximum and enhanced fluorescence compared to their monomeric form in methanol. This spectral behavior aligns with the predictions of the molecular exciton model and indicates the formation of H-type aggregates through intermolecular hydrogen bonding and π-π stacking interactions. Raman spectroscopy further confirms aggregation by revealing two newly enhanced low-frequency bands at 155 and 220 cm^{-1}, corresponding to intermolecular vibrational modes. These observations are consistent with the Aggregation-Enhanced Raman Scattering (AERS) theory, which attributes the enhancements to increased polarizability and excitonic coupling within the aggregates. In addition to low-frequency features, high-frequency Raman bands associated with the monomeric form also show selective enhancement, attributed to Herzberg-Teller vibrational coupling. The result in our study indicates that 4-Mpy molecules in water self-assemble into H-type aggregates, possibly in the form of helical chain conformations.

Keywords

4-Mpy, Molecular Aggregation, AERS, Molecular Exciton Model

1. Introduction

The structure and the spectral properties of molecular aggregates are subjects of intense interest. At its most basic level, it provides an opportunity to examine the intermolecular forces through which the molecules self-assemble to form aggregates. At its most sophisticated level, interest in aggregates is derived from the realization that aggregated molecules play crucial roles in nature, such as light harvesting and the primary charge-separation steps in photosynthesis [1]-[4]. In addition, molecular aggregates have important potential in technological applications. Aggregates formed from molecular aggregates have been used as thin film transistors, spectral sensitizers, organic photoconductors, photothermal therapy, optical probes in biological and synthetic membrane systems, photo-polymerization initiators and, recently, in photothermal therapy (PT) for cancer treatment [5]-[14].

The primary mechanism through which molecules aggregate is self-assembly guided by intrinsic intermolecular interactions. Detailed studies on molecular aggregation through self-assembly and its spectral characterization were advanced by Kasha in his proposed molecular exciton model [15]-[17]. This model classifies the aggregates as either J-type or H-type, depending on the specific alignment of their individual molecular units (monomers). In J-aggregates, molecules self-assemble through end-to-end stacking, resulting in an in-line interaction of their induced dipole moments. In contrast, H-aggregates of molecules self-assemble via plane-to-plane stacking, leading to a parallel alignment of the induced dipole moments. The formation of these types of aggregates has previously been observed in various molecules, including cyanine and xanthene dyes, polycyclic aromatics, and N-protonated porphyrins [18]-[21].

The molecular exciton model, which characterizes J- and H-type aggregates, proposes that interactions between the induced dipole moments in aggregated structures lead to the formation of new exciton states. These exciton states are energetically shifted—lower in J-aggregates and higher in H-aggregates—relative to the monomer's first excited state. As a result, J-aggregates exhibit a red shift, with maximum absorption shifting to longer wavelengths, whereas H-aggregates show a blue shift, with maximum absorption moving to shorter wavelengths. The molecular exciton model has successfully explained fluorescence emission, absorption band frequency shifts, as well as selection rules for electronic transitions between different excitonic states of molecular aggregates.

More recently, Akins et al. introduced a theoretical framework known as Aggregation-Enhanced Raman Scattering (AERS), which analyzes the vibrational characteristics of molecular aggregates in Raman spectroscopy [22]-[24]. This theory extends the molecular exciton model by incorporating its principles to explain the observed Raman enhancements in aggregated species relative to their monomeric counterparts. According to this theory, aggregation of molecules results in enhanced polarizability of the resultant structure, allowing stronger coupling with the incident radiation than is the case for monomeric species. Upon excitation, the aggregate can support the formation of molecular excitonic states. For Raman scattering, the existence of excitonic states as well as the coupling between them create more energy states of the aggregate, generating an enhancement of the Raman signals. This theory predicts the emergence of low-frequency enhanced vibrational modes (lattice modes) due to intermolecular vibrations in the Raman spectrum of aggregates. These bands are enhanced due to nonzero overlap in integral products between the excited states of the aggregates and the ground states of the monomeric species. Additionally, the theory evinces the enhancement of high-frequency Raman bands associated with the monomers, which appear alongside the low-frequency Raman bands of the aggregates. The enhancement of these high-frequency Raman bands is primarily attributed to Herzberg-Teller vibrational coupling between the vibrational and the electronic transitions in the aggregates. This vibrational coupling enables intensity borrowing from allowed transitions, leading to the enhancement of monomer vibrational modes.

In this study, we investigate the spectral property of 4-Mpy aggregates in aqueous solution. We employ solution-driven aggregation of 4-Mpy in water, taking advantage of the low solubility of this molecule in this medium. Our study demonstrates that the absorption maximum of 4-Mpy aggregates exhibits a shift toward shorter wavelengths (a blue shift) and shows enhanced fluorescence relative to the monomeric form of the molecule. By utilizing the spectral analysis of molecular aggregates forwarded by the molecular exciton model, we show that 4-Mpy most likely self-assemble into H-type aggregates through hydrogen bonding and π-π (van der Waals) stacking between their pyridine rings. This study further examines the Raman vibrational characteristics of 4-Mpy aggregates using Raman spectroscopy. Our study reveals the emergence of two new intense low-frequency bands corresponding to intermolecular vibrations of 4-Mpy aggregates, along with enhanced high-frequency Raman bands associated with 4-Mpy monomers, as predicted by the theory of AERS.

2. Experimental Methods

2.1. Chemicals

4-Mercaptopyridine (96%) was purchased from Acros Organics and used without further purification. Methanol was purchased from Fisher Scientific.

2.2. Instrumentation

A solution of 4-MPy was prepared by dissolving 4-Mpy powder in pure methanol and in deionized (DI) water at a 1 mM concentration. A 1 cm path length cuvette was used for UV-Vis measurements. All absorption spectra were recorded using a Perkin-Elmer Lambda 19 UV-vis-near IR spectrometer. All fluorescence spectra were recorded using a Hitachi F-2500 FL Spectrophotometer. Excitation at 340 nm was used to measure the fluorescence of 4-Mpy dissolved in methanol. Excitation at 320 nm was used to measure the fluorescence of 4-Mpy in water. The Raman spectra of 4-Mpy were investigated using Spectra Pro 2750 (0.75 m Triple Grating Monochromator, 1200 gratings/Spectrograph) at the excitation wavelength of 514.5 nm obtained from an Ar^+ laser (Spectra Physics). The Raman spectra of liquid 4-Mpy samples were acquired by depositing a few drops of these samples on a glass surface. The Raman spectra of the 4-Mpy powder sample were obtained by placing the solid powder onto a glass surface. The laser was focused on the sample by using a 100× objective lens attached to a confocal microscope, and the power of the laser on stage was 0.56 mW. The laser spot size was 2 μm, and the slit width was 20 μm. The Raman measurement of the sample was taken with 5 accumulations over a 10 s acquisition. To ensure that the obtained spectra were comparable, the settings, including laser power and exposure time, were all kept constant. The silicon line at 520 nm was used to calibrate the observed wavenumbers. The Raman spectra of the droplets represent the bulk solution.

3. Result and Discussion

3.1. Absorption and Fluorescence Spectroscopy of 4-Mpy

The absorption spectra of 4-Mpy in methanol and water are displayed in **Figure 1**. 4-Mpy dissolved in methanol has a maximum absorption (λ_{max}) at 338 nm, whereas 4-Mpy prepared in water has a maximum absorption (λ_{max}) at 324 nm.

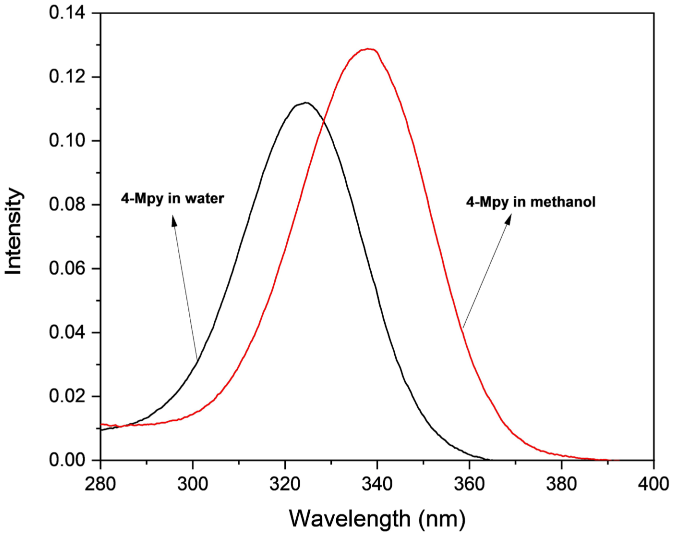

Figure 1. Absorption spectra of 4-Mpy in water (black) and methanol (red). Note: the intensity of the 4-Mpy in water has been adjusted to clearly illustrate the spectral differences.

It is clear from the figure that the maximum absorption band of 4-Mpy shifted to shorter wavelengths (blue shift) as the solvent used to prepare the 4-Mpy solution was changed from methanol to water. This shift in the absorption band can be attributed to the changing polarity of the solvent. However, molecular aggregation through self-assembly due to intermolecular forces cannot be ruled out as a potential cause of this spectral shift.

4-Mpy is highly soluble in methanol but has very low solubility in water. Thus, in methanol, the molecule is expected to remain predominantly in its monomeric form, whereas in water, it is more likely to self-assemble into molecular aggregates due to the unfavorable solvation environment. Indeed, previous studies investigating the aggregation property of 4-Mpy have shown that this molecule aggregates, forming helical chains through self-assembly using hydrogen bonding [25] [26].

In this study, we examined the formation of 4-Mpy aggregates in water by first preparing an initial solution of 4-Mpy in pure methanol. The solvent composition of this initial solution was then changed by gradually adding water to the solution. In this study, the spectral shift of the absorption band of 4-Mpy was monitored as the water content in the initial solution gradually increased. The results of this study are presented in **Figure 2**.

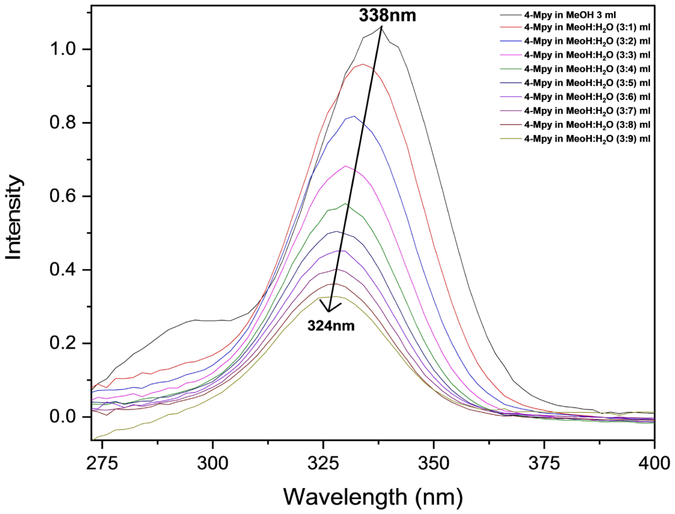

Figure 2. The blue shift in the absorption spectra of 4-Mpy as the initial solvent was gradually changed from pure methanol to mostly water.

The results show a blue shift in the absorption band of 4-Mpy from 338 nm to 324 nm as the solution composition gradually changed from pure methanol to predominantly water.

According to the molecular exciton model, the observed blue shift in the absorption spectra of 4-Mpy in water is due to the formation of H-type molecular aggregates through intermolecular interactions of this molecule. Previous X-ray diffraction studies on 4-Mpy aggregates have shown that the molecule can self-assemble into elongated helical chains through intermolecular N-H…S hydrogen bonding between pyridine rings [25]. These helical chains further organize into three-dimensional structures stabilized by C-H…S hydrogen bonds, C-H…π interactions, and π-π (van der Waals) stacking. It is therefore possible that, in aqueous solution, 4-Mpy molecules form H-aggregates through a similar self-assembly mechanism, leading to the observed spectral blue shift. In addition, **Figure 2** shows a reduction in the intensity of the 4-Mpy absorption band along with the blue shift. This reduction in spectral intensity has been attributed to the formation of molecular aggregates in solution (hypochromic effect) by the exciton model. It is also possible that, as 4-Mpy aggregation increased, the resulting aggregates precipitated out of the solution, thereby contributing to the reduction in intensity of the 4-Mpy absorption band.

To further examine the aggregation of 4-Mpy in water, we conducted a fluorescence study of this molecule in water and methanol. Our study shows that 4-Mpy in water exhibits a relatively strong fluorescence band at 514 nm (**Figure 3(a)**), whereas in methanol this molecule does not show any noticeable fluorescence (**Figure 3(b)**). Previous fluorescence studies on mero-cyanine and hemi-cyanine dyes have reported enhanced fluorescence emission from the H-aggregated structures of these dyes [27]-[29]. The authors of these studies attributed the enhanced fluorescence to the rigidified structure of these cyanine dyes induced by their aggregation. Their studies showed that the monomeric forms of these dyes exhibit very weak fluorescence due to a bond-twisting mechanism that activates non-radiative decay pathways, leading to reduced fluorescence intensity.

The authors concluded that these nonradiative deactivation channels are suppressed due to the formation of the cyanine dye aggregates, causing the aggregates to fluoresce. The fluorescence characteristic of the 4-Mpy aggregates in this study is consistent with that previously observed for cyanine dye aggregates. Results from this study provide further evidence that 4-Mpy molecules are likely to form H-aggregates in aqueous solutions, while in methanol they primarily remain as free molecules.

3.2. Raman Spectroscopy of 4-Mpy

A comparison of the Raman spectra of 4-Mpy molecules in water and methanol is presented in **Figure 4**. A Raman spectrum of the 4-Mpy solid powder is also included in the figure for reference purposes. The figure shows that the Raman spectrum of 4-Mpy molecules in water is dominated by strong enhancements of three bands at 155, 220, and 475 cm^{-1}. Upon close examination of the figure, we can see that the two enhanced bands at 155 and 220 cm^{-1} are new bands which are absent in the Raman spectra of 4-Mpy in methanol and in solid powder. According to the theory of AERS, these newly enhanced low-frequency Raman bands (lattice modes)

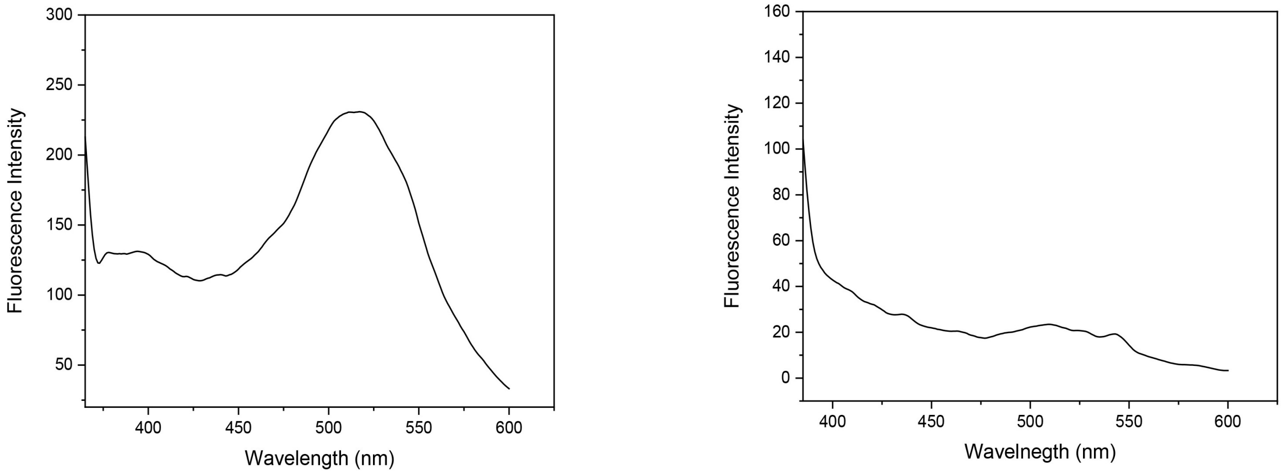

(a)

(b)

Figure 3. (a): Fluorescence spectrum of 4-Mpy in water (left); (b): Fluorescence spectrum of 4-Mpy in methanol (right).

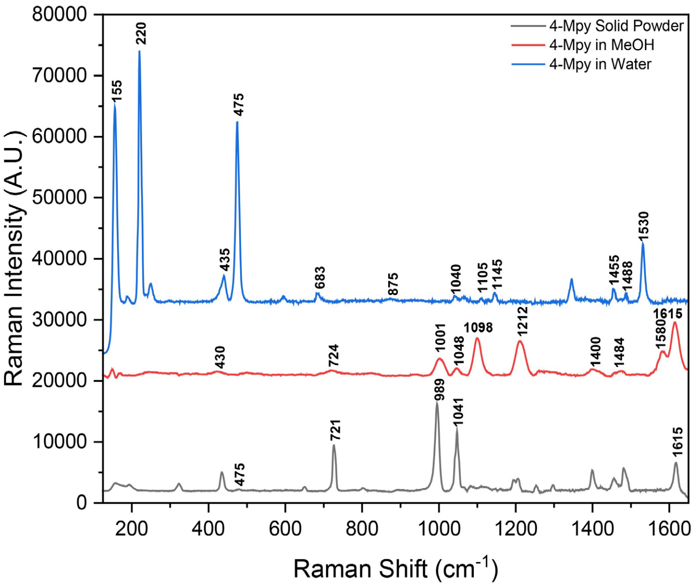

Figure 4. Raman spectra of 4-Mpy in water (blue), methanol (red), and solid powder (black). Excitation is at 514.5 nm. The baseline was subtracted from all three Raman spectra using Origin graphing software 2022.

arise from intermolecular vibrations, indicating the formation of 4-Mpy aggregates in water. The enhancements of the low-frequency Raman bands are enabled by the increased polarizability of the aggregated structure and the coupling between excitonic states formed upon aggregation. The appearance of these new low-frequency Raman bands confirms the prediction proposed by the theory of AERS.

In addition, the Raman spectrum of 4-Mpy in water also shows bands above 400 cm^{-1} associated with the vibrations of the 4-Mpy monomers. These high-frequency bands can also be seen in the Raman spectrum of 4-Mpy in methanol and in solid powder. The correlated Raman band positions and their vibrational assignments are shown in Table 1.

Among the high-frequency bands, the most enhanced band appears at 475 cm^{-1}, followed by the band at 1530 cm^{-1}. Both bands appear very weak in the Raman spectra of 4-Mpy in methanol and in solid powder. The enhancement of these bands is attributed to Herzberg-Teller intensity borrowing, through which vibrational modes of the monomer gain increased intensity.

The figure also shows reduced intensity of some of the Raman bands at 721, 989, 1041, and 1615 cm^{-1} in the Raman spectrum of the 4-Mpy in water. These bands appear to have strong intensity in the Raman spectrum of 4-Mpy in solid powder. It is reasonable to expect that the molecular geometry of 4-Mpy aggregates in water differs from that of 4-Mpy monomers in methanol and in solid powder. As a result, following the theory of AERS, the symmetry elements of the aggregates follow selection rules that differ from those of the monomeric species, contributing to variations in Raman intensity. Similar conclusions have also been drawn in analyses of Raman intensity differences between cyanine aggregates and their monomeric forms [30] [31].

Table 1. Column 1 contains the assignments from references [32]-[34]. Columns 2 and 3 are from this work.

Assignment	4-*MPy Powder*	4-*MPy Methanol*	4-*MPy Water*
Lattice mode (aggregate)			155
Lattice mode (aggregate)			220
7a (C-S in-plane deformation/C-C-C out-of-plane deformation)	435	430	435
16b (C-C-C out-of-plane deformation)	475		475
6b (C-C-C bending)	655		683
6a (in-plane ring deformation, C=S)	721	724	
out-of-plane N-H def	870		875
1a (ring breathing)	989	1001	
18a (in-plane C-H def.)	1041	1048	1040
12a (trigonal ring breathing with C=S)	1107	1098	1105
15b (C-H def)	1150		1145
9a (in-plane C–H def.)	1200	1212	
14b (ring stretch)	1396	1400	
19b (ring stretch)	1457		1455
19a (ring stretch)	1470	1484	1488
19a (ring stretch)	1525		1530
8b (ring stretch with deprotonated nitrogen)	1580	1580	
8a (ring stretch)	1615	1615	

The results of this study strongly suggest the formation of 4-Mpy aggregates in water. In previous studies of the Cyanine dye aggregates, the emergence of two intense low-frequency Raman bands was attributed to the existence of two different types of aggregates [31]. The fact that the Raman spectrum of 4-Mpy shows enhancements of two low-frequency bands indicates the existence of two types of H-aggregates. Indeed, previous studies of 4-Mpy aggregates reported the existence of two types of helical chain conformations—a left-handed helix and a right-handed helix [25]. Therefore, it is possible that 4-Mpy in water aggregates to form two different helical structures, resulting in the enhancements of two intense low-frequency Raman bands.

Acknowledgements

We are indebted to the National Science Foundation (CHE-1402750) for partial funding of this project. This work was also partially supported by NSF grant number HRD-1547830 (IDEALS CREST).

Conflicts of Interest

The authors declare that they have no known competing financial interests or personal relationships that could have appeared to influence the work reported in this paper.

References

[1] Pearlstein, R.M. (1987) Photosynthesis. Elsevier Science, Amsterdam, p. 299.

[2] Warshel, A. and Parson, W.W. (1987) Spectroscopic Properties of Photosynthetic Reaction Centers. 1. Theory. *Journal of the American Chemical Society*, **109**, 6143-6152. https://doi.org/10.1021/ja00254a039

[3] Creighton, S., Hwang, J.K., Warshel, A., Parson, W.W. and Norris, J. (1988) Simulating the Dynamics of the Primary Charge Separation Process in Bacterial Photosynthesis. *Biochemistry*, **27**, 774-781. https://doi.org/10.1021/bi00402a043

[4] Michel-Beyerle, M.E., Plato, M., Deisenhofer, J., Michel, H., Bixon, M. and Jortner, J. (1988) Unidirectionality of Charge Separation in Reaction Centers of Photosynthetic Bacteria. *Biochimica et Biophysica Acta* (*BBA*)—*Bioenergetics*, **932**, 52-70. https://doi.org/10.1016/0005-2728(88)90139-9

[5] Briseno, A.L., Roberts, M., Ling, M., Moon, H., Nemanick, E.J. and Bao, Z. (2006) Patterning Organic Semiconductors Using "Dry" Poly(Dimethylsiloxane) Elastomeric Stamps for Thin Film Transistors. *Journal of the American Chemical Society*, **128**, 3880-3881. https://doi.org/10.1021/ja058226v

[6] Gilman, R. (1974) Progress Report of Geologic Mapping in the Ellsworth, Great Pond, Lead Mountain, Tug Mountain, and Wesley quadrangles, Maine. M*aine Geological Survey Publication*, *Progress Report*, **18**, 418.

[7] Borsenberger, P.M., Chowdry, A., Hoesterey, D.C. and Mey, W. (1978) An Aggregate Organic Photoconductor. II. Photoconduction Properties. *Journal of Applied Physics*, **49**, 5555-5564. https://doi.org/10.1063/1.324476

[8] Waggoner, A. (1976) Optical Probes of Membrane Potential. *The Journal of Membrane Biology*, **27**, 317-334. https://doi.org/10.1007/bf01869143

[9] Chatterjee, S., Davis, P.D., Gottschalk, P., Kurz, M.E., Sauerwein, B., Yang, X., *et al.* (1990) Photochemistry of Carbocyanine Alkyltriphenylborate Salts: Intra-Ion-Pair Electron Transfer and the Chemistry of Boranyl Radicals. *Journal of the American Chemical Society*, **112**, 6329-6338. https://doi.org/10.1021/ja00173a022

[10] Hanamura, E. (1988) Very Large Optical Nonlinearity of Semiconductor Microcrystallites. *Physical Review B*, **37**, 1273-1279. https://doi.org/10.1103/physrevb.37.1273

[11] Sasaki, F. and Kobayashi, S. (1993) Anomalous Excitation Density Dependence of Nonlinear Optical Responses in Pseudoisocyanine *J* Aggregates. *Applied Physics Letters*, **63**, 2887-2889. https://doi.org/10.1063/1.110315

[12] Wang, Y. (1986) Efficient Second-Harmonic Generation from Low-Dimensional Dye Aggregates in Thin Polymer Film. *Chemical Physics Letters*, **126**, 209-214. https://doi.org/10.1016/s0009-2614(86)80041-0

[13] Wang, Y. (1991) Resonant Third-Order Optical Nonlinearity of Molecular Aggregates with Low-Dimensional Excitons. *Journal of the Optical Society of America B*, **8**, 981-985. https://doi.org/10.1364/josab.8.000981

[14] Xu, J., Yin, Z., Zhang, L., Dong, Q., Cai, X., Li, S., *et al.* (2022) Hydrogen-Bonding-Induced H-Aggregation of Charge-Transfer Complexes for Ultra-Efficient Second Near-Infrared Region Photothermal Conversion. *CCS Chemistry*, **4**, 2333-2343. https://doi.org/10.31635/ccschem.021.202101058

[15] Kasha, M. (1963) Energy Transfer Mechanisms and the Molecular Exciton Model for Molecular Aggregates. *Radiation Research*, **20**, 55-70.

https://doi.org/10.2307/3571331

[16] Kasha, M. (1959) Relation between Exciton Bands and Conduction Bands in Molecular Lamellar Systems. *Reviews of Modern Physics*, **31**, 162-169. https://doi.org/10.1103/revmodphys.31.162

[17] Kasha, M., Rawls, H.R. and Ashraf El-Bayoumi, M. (1965) The Exciton Model in Molecular Spectroscopy. *Pure and Applied Chemistry*, **11**, 371-392. https://doi.org/10.1351/pac196511030371

[18] Herz, A.H. (1977) Aggregation of Sensitizing Dyes in Solution and Their Adsorption onto Silver Halides. *Advances in Colloid and Interface Science*, **8**, 237-298. https://doi.org/10.1016/0001-8686(77)80011-0

[19] Selwyn, J.E. and Steinfeld, J.I. (1972) Aggregation of Equilibriums of Xanthene Dyes. *The Journal of Physical Chemistry*, **76**, 762-774. https://doi.org/10.1021/j100649a026

[20] Heesemann, J. (1980) Studies on Monolayers. 1. Surface Tension and Absorption Spectroscopic Measurements of Monolayers of Surface-Active Azo and Stilbene Dyes. *Journal of the American Chemical Society*, **102**, 2167-2176. https://doi.org/10.1021/ja00527a004

[21] Akins, D.L., Zhu, H. and Guo, C. (1994) Absorption and Raman Scattering by Aggregated Meso-Tetrakis(P-Sulfonatophenyl)Porphine. *The Journal of Physical Chemistry*, **98**, 3612-3618. https://doi.org/10.1021/j100065a012

[22] Akins, D.L. (1986) Theory of Raman Scattering by Aggregated Molecules. *The Journal of Physical Chemistry*, **90**, 1530-1534. https://doi.org/10.1021/j100399a014

[23] Akins, D.L. and Lombardi, J.R. (1987) Excitation Wavelength Dependence of Enhanced Raman Bands of Aggregated Molecules. *Chemical Physics Letters*, **135**, 495-500. https://doi.org/10.1016/0009-2614(87)85198-9

[24] Akins, D.L. (2014) Enhanced Raman Scattering by Molecular Nanoaggregates. *Nanomaterials and Nanotechnology*, **4**, 4. https://doi.org/10.5772/58403

[25] Muthu, S. and Vittal, J.J. (2004) A New Polymorph of 4-Pyridinethione Containing a Helical Assembly Based on N-H···S Hydrogen Bonds. *Crystal Growth & Design*, **4**, 1181-1184. https://doi.org/10.1021/cg0498812

[26] Etter, M.C., MacDonald, J.C. and Wanke, R.A. (1992) Solution and Solid-State Aggregation Properties of 4-Mercaptopyridine-4-Thiopyridone. *Journal of Physical Organic Chemistry*, **5**, 191-200. https://doi.org/10.1002/poc.610050404

[27] Rösch, U., Yao, S., Wortmann, R. and Würthner, F. (2006) Fluorescent H-Aggregates of Merocyanine Dyes. *Angewandte Chemie International Edition*, **45**, 7026-7030. https://doi.org/10.1002/anie.200602286

[28] Lu, L., Lachicotte, R.J., Penner, T.L., Perlstein, J. and Whitten, D.G. (1999) Exciton and Charge-Transfer Interactions in Nonconjugated Merocyanine Dye Dimers: Novel Solvatochromic Behavior for Tethered Bichromophores and Excimers. *Journal of the American Chemical Society*, **121**, 8146-8156. https://doi.org/10.1021/ja983778h

[29] Zeena, S. and Thomas, K.G. (2001) Conformational Switching and Exciton Interactions in Hemicyanine-Based Bichromophores. *Journal of the American Chemical Society*, **123**, 7859-7865. https://doi.org/10.1021/ja010199v

[30] Akins, D.L., Zhuang, Y.H., Zhu, H.R. and Liu, J.Q. (1994) Raman Excitation Spectra of Exciton-Phonon Modes of Aggregated 2,2'-Cyanine Using an Internal Raman Standard. *The Journal of Physical Chemistry*, **98**, 1068-1072. https://doi.org/10.1021/j100055a005

[31] Akins, D.L., Özçelik, S., Zhu, H. and Guo, C. (1997) Aggregation-Enhanced Raman

Scattering of a Cyanine Dye in Homogeneous Solution. *The Journal of Physical Chemistry A*, **101**, 3251-3259. https://doi.org/10.1021/jp963122f

[32] Baldwin, J.A., Vlčková, B., Andrews, M.P. and Butler, I.S. (1997) Surface-Enhanced Raman Scattering of Mercaptopyridines and Pyrazinamide Incorporated in Silver Colloid-Adsorbate Films. *Langmuir*, **13**, 3744-3751. https://doi.org/10.1021/la960719d

[33] Hu, J., Zhao, B., Xu, W., Li, B. and Fan, Y. (2002) Surface-Enhanced Raman Spectroscopy Study on the Structure Changes of 4-Mercaptopyridine Adsorbed on Silver Substrates and Silver Colloids. *Spectrochimica Acta Part A*: *Molecular and Biomolecular Spectroscopy*, **58**, 2827-2834. https://doi.org/10.1016/s1386-1425(02)00074-4

[34] Wang, Z. and Rothberg, L.J. (2005) Origins of Blinking in Single-Molecule Raman Spectroscopy. *The Journal of Physical Chemistry B*, **109**, 3387-3391. https://doi.org/10.1021/jp0460947